Curvature Based Mobility Analysis and Form Closure of Smooth Planar Curves with Multiple Contacts

Ramakrishna K, Dibakar Sen

Abstract

This paper presents a simple second order, curvature based mobility analysis of planar curves for rotation. The underlying theory and methods are purely geometrical, dealing with penetration and separation of curves with multiple contacts, based on relative configuration of osculating circles at points of contact for rotation about each point of the plane. Starting with a single contact, partitioning of the plane into four types of mobility regions has been shown. Using point based composition operations based on dual-number matrices; analysis has been extended to computationally handle multiple contacts scenario. A novel coloured directed line has been proposed to capture the contact scenario. Multiple contacts mobility is obtained through intersection of the mobility half spaces. It is derived that mobility region comprise a pair of open or a single closed convex polygon. The theory has been used for analysis of form closure and synthesis of revolute pairs.

Keywords: mobility analysis, form closure, kinematic pair.

1 Introduction

The study of mobility analysis of objects in contact dates back to the time of Franz Reuleaux [1]. Planar constraints were analyzed by velocity centers, which is a first order analysis. Reuleaux's method sometimes gives false positives [2], [3], [4]. It is recognized in literature that the first order mobility analysis, which considers only the tangent at the point of contact, is insufficient [3], [4], [5] to give complete information regarding the relative motion between two rigid bodies in contact, especially when persistence of contact between the two is not insisted upon. A second order analysis of curves and surfaces in the configuration space characterizing the mobility of the concerned bodies is available in [3]. The approach is insightful but is rather involved for practical use. The work presented here uses geometry of the objects directly. Mobility analysis of objects in contact is presented in section 2. Section 3 deals with region based composition operations. Extension of mobility analysis to the form closure of a planar object has been worked out in section 4. Synthesis of revolute kinematic pair based on the mobility analysis developed, is presented in section 5.

Ramakrishna K
Department of Mechanical Engineering, Indian Institute of Science, Bangalore-560012.
E-mail: ram.itbhu@gmail.com.

Dibakar Sen
Department of Mechanical Engineering, Indian Institute of Science, Bangalore-560012.
E-mail: sendibakar1@gmail.com.

2 Mobility Analysis

The mobility analysis in this paper deals with the ability of a smooth planar object initially having finite number of contacts with a fixed object, to rotate about an arbitrary point of the plane. All the contacts are unilateral constraints disallowing penetration into fixed planar object. The motion space of an object having multiple contacts with a fixed object is studied in the following sections.

2.1 Representation of planar objects

The planar smooth objects are represented using NURB curves which offer a variety of shapes. The *first derivatives* of the curves give the tangent vectors, which are then used for appropriately aligning the two bodies in a contacting configuration. The *second derivative*s at the contact give the osculating circles which closely approximate the curves at that point. The fixed and moving curves and their osculating circles are referred to as, *f*-curve, *m*-curve, *f*-circle and *m*-circle respectively. The centers of *f*- and *m*-circles are C_f and C_m respectively. The three possible types of contacting geometries shown in Fig.1 belong to two classes which we call convex and concave class. In a convex type contact both the contacting curves are convex and in a concave type contact one of the contacting curves is of concave type. We refer to the contact normal line as n-line in this paper.

2.2 Single contact mobility analysis

The canonical aspect of mobility analysis of objects in contact is determining the mobility characteristics for a single contact. Any point O in the plane is considered and the *m*-curve is given a small rotation about this point; the penetration or separation resulting from this motion is analyzed using the *f*- and *m*-circles. The penetration and separation of *m*-circle for a clockwise (CW) and counterclockwise (CCW) rotation about various locations of rotation center O in the plane, for a convex contact is shown in Fig.2. The centers of transformed *m*-circle after CCW and CW rotation are C'_m and C''_m respectively.

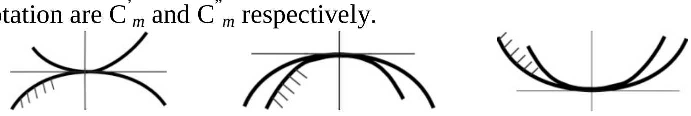

(a) Convex (*m*)-Convex (*f*) contact. (b) Concave (*m*)-Convex (*f*) contact. (c) Convex (*m*)-Concave (*f*) contact.

Fig.1: Geometries of contacting curves.

2.2.1 Geometrical analysis

We now give a geometrical proof of penetration or separation for two cases to put forward the line of argument, which is also applicable to all the other cases too. The geometrical proof of penetration or separation is simple if the center of rotation lies along the n-line. For the case in Fig.2 (c) (left figure), using triangle inequality in triangle OC'_mC_f ; we have $C_f C'_m + C'_m O > OC_f$. But we have $OC_f = OC_m + C_mC_f$ and also since O is the center of rotation; $OC_m = OC'_m$. Hence we have $C_f C'_m > C_mC_f$, which means that the center to center distance between the transformed *m*-circle after a CCW rotation and *f*-circle increased. This implies that the *m*-circle separates from *f*-circle for a CCW rotation about O. When the center of rotation doesn't lie along the n-line, an additional geometrical construction is required. In Fig.2 (a), perpendicular bisector to the line-segment $C_mC^{''}_m$ is dropped from rotation center O. This perpendicular bisector cuts the line-joining the original centers of curvature in T. Now in triangle $C^{''}_mC_fT$, we have $C_fT + TC^{''}_m > C^{''}_mC_f$. But $TC^{''}_m = TC_m$ since T lies on the perpendicular bisector of the line-segment $C_mC^{''}_m$. Hence, $C_fT+TC_m > C^{''}_mC_f$, meaning $C_f C_m > C^{''}_mC_f$ and implying that *m*-circle penetrates into the *f*-circle for a CW rotation about point O.

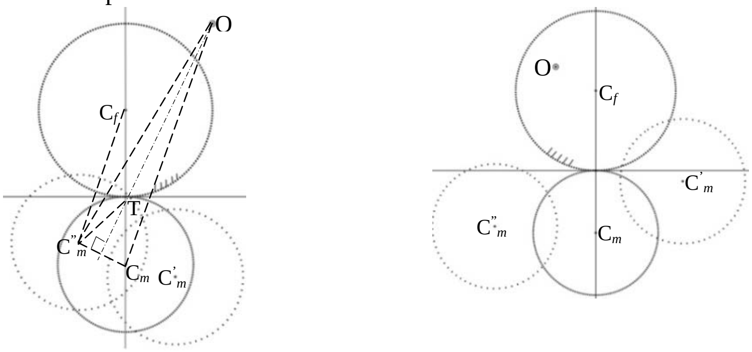

(a) O in right-half plane. CCW-separation. CW-penetration.

(b) O in left-half plane. CCW-penetration. CW-separation.

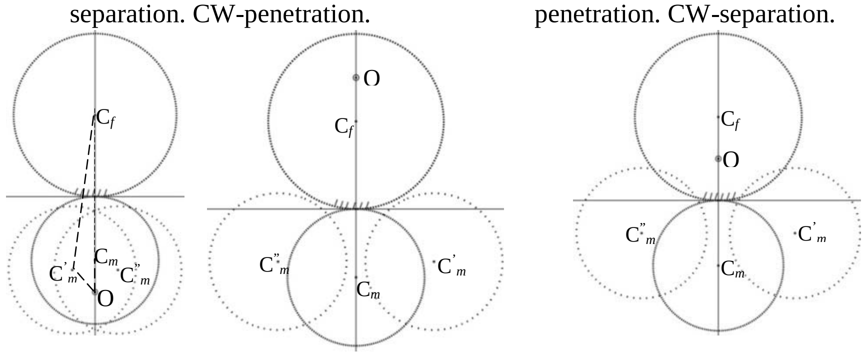

(c) O not in between C_f and C_m along n-line. CCW and CW- separation.

(d) O in between C_f and C_m along n-line. CCW and CW- penetration.

Fig.2: Transformation of *m*-circle after CCW and CW rotation about point O in the plane for a convex contact.

2.2.2 Partitioning of the plane

At any point of contact, the plane is partitioned into four regions based on the *mobility characteristics* of the *m*-curve with respect to the *f*-curve as shown in Fig.3. For a point in region 1, the *m*-circle penetrates into *f*-circle for both clockwise (CW) and counterclockwise (CCW) rotation and hence this is a blocked region. Region 2 contains points for which *m*-circle penetrates into *f*-circle for clockwise rotation, but separates for counterclockwise rotation. In mobility region 3, the situation is opposite. In region 4, *m*-circle separates from *f*-circle for both directions of rotation. Regions 1 and 4 are line segments which are the partitions of the n-line; regions 2 and 3 are the two half-planes on either side of the n-line. The region delimited by the centers of curvature is either region 1 or region 4 depending on the geometry of curves at the contact. The complementary region on the line is of the alternate type as shown in Fig.3. If the rotation center coincides with either C_f or C_m, the contact between the curves will be preserved for second-order rotation motion about this point, thus *m*-curve remains adhered to the *f*-curve. While the motion of *m*-curve for rotation about C_m is pure slipping at contact point, motion of *m*-curve for rotation about C_f is a pure sliding one.

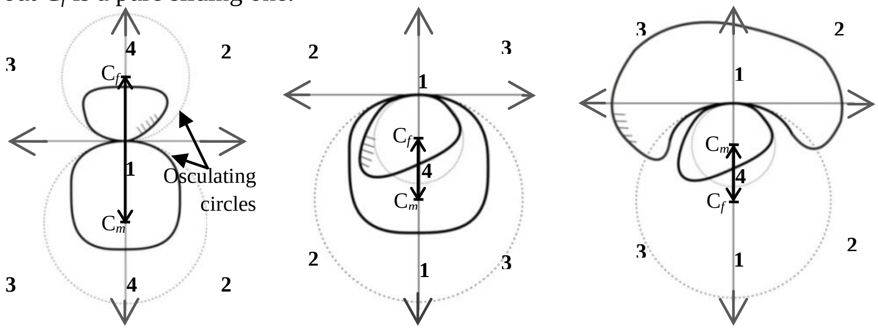

(a) Convex contact. (b) Concave contact with moving concave curve. (c) Concave contact with fixed concave curve.

Fig.3: Motion space from contact point curvatures for various contacting geometries. Regions 1: No rotation blocked, 2: CW rotation blocked, 3: CCW rotation blocked, 4: Every rotation blocked.

It is thus well established from the above observations that the relative configuration of the two centers of curvature and the point of contact identify the four regions unambiguously. *The motion space partition doesn't depend on the actual position of contact point; it depends only on the absolute location of centers of curvature and the relative location of contact point with respect to the line-segment delimited by the two centers of curvature*. Each point in region 1, 2, 3 and 4 is color coded as red (*R*), green (*G*), yellow (*Y*) and white (*W*) respectively for computer visualization and from now the four region numbers and four colors are used interchangeably.

2.2.3 Computational scheme

A point classification scheme has been developed to computationally handle coloring of the plane for a single contact. The position vectors of the point of contact (C) and a point O in the plane are $\boldsymbol{C}$ and $\boldsymbol{O}$ respectively. $\boldsymbol{C_m}$ and $\boldsymbol{C_f}$ are the position vectors of centers of curvature C_m and C_f respectively. We define $\boldsymbol{R_m} = \boldsymbol{C_m}-\boldsymbol{C}$, $\boldsymbol{R_f} = \boldsymbol{C_f}-\boldsymbol{C}$ and $\boldsymbol{p} = \boldsymbol{O}-\boldsymbol{C}$ (Fig.4). $\boldsymbol{k}$ is unit vector pointing out of the plane of the paper.

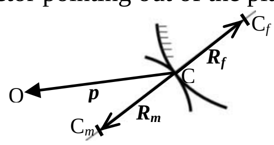

Fig.4: Vectors used, to classify a point (O) of the plane.

Point O in the plane is classified to which region it belongs to, based on the following rules: (i). if $(\boldsymbol{R}_m \bullet \boldsymbol{R}_f)(((\boldsymbol{R}_m - \boldsymbol{R}_f)\times \boldsymbol{p})\bullet \boldsymbol{k}) < 0$, the point belongs to region 2(*G*), with respect to that contact. (ii). if $(\boldsymbol{R}_m \bullet \boldsymbol{R}_f)(((\boldsymbol{R}_m - \boldsymbol{R}_f)\times \boldsymbol{p})\bullet \boldsymbol{k}) < 0$, the point belongs to region 3(*Y*), with respect to that contact. (iii). if $(\boldsymbol{R}_m \bullet \boldsymbol{R}_f)(((\boldsymbol{R}_m - \boldsymbol{R}_f)\times \boldsymbol{p})\bullet \boldsymbol{k}) = 0$, then point lies along the n-line. To further classify a point lying on the n-line, we define a scalar *r* such that

$$r = \frac{\left(\left(\boldsymbol{C}_m - \boldsymbol{O}\right)\bullet \boldsymbol{R}_m\right)\left(\left(\boldsymbol{C}_f - \boldsymbol{O}\right)\bullet \boldsymbol{R}_f\right)}{\left(\left(\boldsymbol{R}_m - \boldsymbol{R}_f\right)\bullet \boldsymbol{R}_m\right)\left(\left(\boldsymbol{R}_m - \boldsymbol{R}_f\right)\bullet \boldsymbol{R}_f\right)} \tag{1}$$

The point belongs to region 1 (*R*) or region 4 (*W*) if $r < 0$ or if $r > 0$ respectively.

2.3 Multiple contacts mobility analysis

If mobility in one sense is disallowed by a contact, no new contact can provide it back. Hence, the net mobility is the intersection of mobility obtained with respect to each contact. The composition rules in terms of color codes are: (*a*). $R \oplus R = R$, (*b*). $G \oplus G = G$, (*c*). $Y \oplus Y = Y$, (*d*). $Y \oplus R = R = R \oplus Y$, (*e*). $G \oplus Y = R = Y \oplus G$, (*f*). $Y \oplus W = Y = W \oplus Y$, (*g*). $G \oplus W = G = W \oplus G$, (*h*). $R \oplus W = R = W \oplus R$. To computationally perform the above compositions, a matrix representation for color codes is proposed. Each color is represented as a 2×2 matrix as

$$R = \begin{pmatrix} 0 & 0 \\ 0 & 0 \end{pmatrix},\ G = \begin{pmatrix} 1 & -\varepsilon \\ \varepsilon & 0 \end{pmatrix},\ Y = \begin{pmatrix} 0 & \varepsilon \\ -\varepsilon & 1 \end{pmatrix} \text{ and } W = \begin{pmatrix} 1 & 0 \\ 0 & 1 \end{pmatrix}$$

where ε is a symbol such that $\varepsilon \neq 0 \,\&\, \varepsilon^2 = 0$. The above representation is only one of the many possible dual-number matrix representations. The composition operation corresponds to a matrix multiplication. Fig.5a and Fig.5b show the mobility regions of the plane for two contacts and three contacts cases respectively, based on point classification scheme.

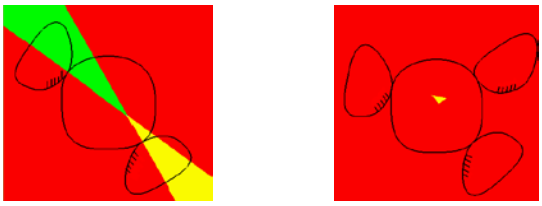

(a) Coloring of the plane for a two contacts case.

(b) Coloring of the plane for a three contacts case.

Fig.5: Motion space of a body with two and three contacts.

2.4 Asymptotic mobility

The above analysis indicates that the mobility based classification of points has coherence in the convex regions; if any point on a line through a point of contact C is considered in the region with some mobility, classification of the points on the two sides of C are opposite. This would imply that the classification of the point at infinity depends on the direction of its approach; this is unacceptable! However, it can be observed that both actually mean that the translational mobility in an orthogonal direction is consistent (Fig.6). Thus, actually there is no ambiguity.

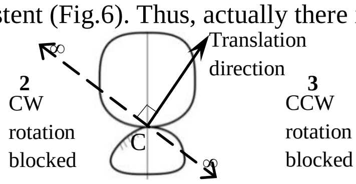

Fig.6: Rotational mobility subsumes translational mobility in the plane.

3 Region Based Composition

Method of computing mobility type classification of a given point of the plane in a multiple contacts scenario was described in section 2.3. But if one asks a question of the kind: “Is there any region/point belonging to region 4 in the plane?”, the computational method described in previous sections fails to answer this question since that procedure samples points of the plane with certain accuracy. In such a kind of point sampling procedure, one may lose out point/s belonging to region 4 since they always exist along lines as delimited line segments or as just points. In a two contacts case like Fig.5a, the point of intersection of two n-lines belongs to region 4 (*W*), but the colored image doesn’t show this because that point missed out in the sampling process. So a thorough region based composing operation scheme is developed.

3.1 Representation of a single contact

Based on the mobility characteristics for a single contact (section 2.2), a representation which combines all the contacting geometry types is proposed, which allows for composing mobility regions in a multiple contacts scenario. Each contact and the corresponding n-line is represented using a colored oriented line-segment whose end points are the centers of curvature C_m and C_f , and its orientation being from C_m towards C_f. *Color code of the line-segment*, either red (*r*) or white (*w*), is appended to the oriented line-segment to represent convex and concave class contact respectively. We use the terminology of *r*-line and *w*-line to mean a n-line containing colored oriented line-segment of red and white color respectively (Fig.7).

(a) *r*-line contact and mobility regions. (b) *w*-line contact and mobility regions.

Fig.7: Mobility regions in a single contact.

The left and right motion half-planes of *r*-line are yellow (*Y*) and green (*G*) respectively (Fig.7a). For a *w*-line, the half-plane colors are swapped (Fig.7b). Along the n-line, if the line-segment is either red (*R*) or white (*W*), the complimentary regions of the line are either white (*W*) or red (*R*) respectively.

3.2 Multiple contacts mobility regions

Mobility regions of a single point contact is a pair of half spaces delineated by the n-line. Each half is a convex set; hence their Boolean composition also constitutes a set of convex regions. In multiple contacts scenario the n-lines intersect to give a set of unbounded and bounded convex cells which are intersections of the half-planes generated by the intersecting lines themselves. The problem of classifying the entire plane is reduced to the classification of edges, vertices and interiors of these convex cells. Based on the discussions above the following observations can be made.

i. In a single contact case, along the n-line, only the symmetric mobility regions 1 and 4 occur. Multiple contacts can only reduce mobility; hence, in a multiple contacts scenario, bidirectional rotation is possible only if
    a. All the n-lines pass through a given point

b. The given point belongs to region 4 for each contact

Result 1: In *a multiple contacts scenario bidirectional rotation is possible only about a single point in the plane.*

ii. Suppose, all but one other n-lines intersect at a point and the point provides mobility type 4 with respect to every contact. Now, this point belongs to one of the half-planes of the non-cointersecting line. As a result, only a net unidirectional mobility would survive.

Result 2: If atleast one of the n-lines does not pass through the point of intersection of any two of other n-lines, then the mobility region 4 is null.

iii. In a single contact case, the unidirectional rotational mobility regions 2 and 3 occur as open half-spaces. Intersection of convex sets is a convex set. Intersection of a set of open halfspaces is a set of bounded or unbounded open regions of coherent mobility classification.

Result 3: A bounded region of mobility and a point of bidirectional mobility are mutually exclusive

Result 4: If a single point has unidirectional mobility then its neghbourhood also has the same mobility (derived from coherence and open nature of set).

Result5: A single point with unidirectional mobility induces a ***finite*** *neighbourhood of same mobility.*

From the above results it is concluded that only two patterns of the configuration of the n-lines are distinctly different, viz. all n-lines are co-intersecting and they are not so. In the first case, if the common point has *bidirectional mobility with respect to all* the contacts, then the pair has instantaneous bidirectional mobility; otherwise, it has no mobility about this point. Additionally, for *n* contacts, the plane is partitioned into *2n* unbounded wedge shaped regions. In the second case, no point in the plane provides bidirectional mobility. Additionally, we get a collection of more than *2n* bounded and unbounded regions wherein the number of unbounded regions is always *2n*. Each of these regions is a convex region containing points with coherent mobility type. Hence classification of any one point classifies all points in the region.

Lemma: *If one of the bounded regions provides non-trivial mobility, then this is the only such region; otherwise it is a pair of disjoint unbounded regions with opposite mobility*.

Proof: Enumeration of all the regions is combinatorially difficult; the region(s) which survive successive inclusion of the n-lines would be the desired region with unidirectional mobility. Thus we need to classify a given region with respect to a newly added n-line. If the new line intersects a region, the subspace with matching classification only survives. If it does not intersect then it will kill the region with opposite classification. Hence, *every new line either reduces the extent or count of the regions with unidirectional mobility*. Since one contact gives two regions of unidirectional mobility, this number is never exceeded. Moreover, since the unbounded regions are convex, open and disjoint, they are always linearly separable. Hence, the line that isolates a bounded region of unidirectional mobility, the other unbounded region would be in the same side of the line but with opposite mobility. Thus it will annihilate the unbounded region. Hence the lemma is proved.

The lemma and its proof provide a highly efficient procedure to determine availability and type of mobility for a pair of smooth curves with n contacts. The algorithm is omitted for the sake of brevity, but one such result is shown in Fig.8. For convenience r-line segment is colored black in the figure.

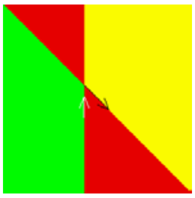

(a) 2nd n-line reduces half plane regions 2 and 3.

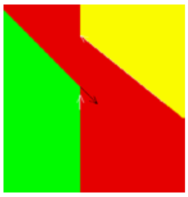

(b) Introducing 3rd n-line reduces extent of region 3.

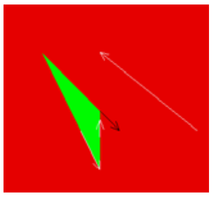

(c) Introducing 4th n-line annihilates region 3.

Fig.8: Successive inclusion of n-lines and unidirectional mobility regions.

4 Form Closure Analysis

A contact configuration for which region 1 covers the whole plane corresponds to a form closure configuration and the object is immobilized. For a contact scenario similar to the one shown in Fig.5a, if a third contact can be established such that the third n-line passes through the point of intersection of previous two n-lines and is contained in the vertically-opposite sections belonging to region 1 as a result of two contact composition, and the point of intersection of these three n-lines after composition for three contacts belongs to region 1, then the entire plane belongs to region 1 as shown in Fig.9 and the object is form closed. Fig.10 illustrates a special situation wherein only two contacts immobilize the m-curve. However, a first order analysis would indicate that the instantaneous center of the moving curve lies anywhere along the n-line. This establishes the simplicity of the present approach and the efficacy of its inferences.

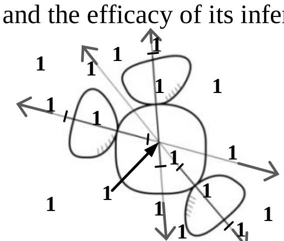

Fig.9: Form closure with three convex fixtures.

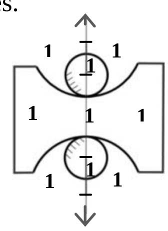

Fig.10: Form closure with two contacts.

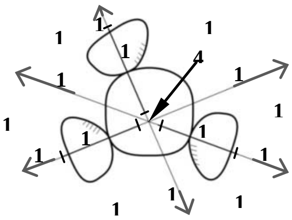

Fig.11: Local bidirectional rotation about intersection point of n-lines.

5 Synthesis of Revolute Pair

In a multiple contacts scenario, if region 4 is not null, then a *local bidirectional rotation* about a point in this region is feasible, and mostly the bodies are going to separate as a result. In the two contacts scenario like the one shown in Fig.5a, only the point of intersection of n-lines belongs to region 4. To preserve this point to region 4 and cover the rest of plane with region 1, a third n-line is introduced such that it passes through the point of intersection of previous two n-lines and is contained in the vertically opposite sections belonging to region 1 of two contact composition and the intersecting point of three lines belongs to region 4 with respect to third contact also (Fig.11). The persistence and change of contacts define different types of revolute kinematic pair with gross motion capabilities and the limits of their ranges of motion respectively. Alternatively, we can also have a persistence of center of rotation by having a *persistence of contact and contacting geometries* (Fig.12) which follows from the observation that in a single contact, rotation about C_f or C_m preserves the contact. The rotation center is then the coincident center of curvature at all the contacts, of the curve along which the point of contact moves. The second-order mobility analysis thus helps one to identify equivalent revolute-joint types resulting from conforming as well as non-conforming geometries in contact.

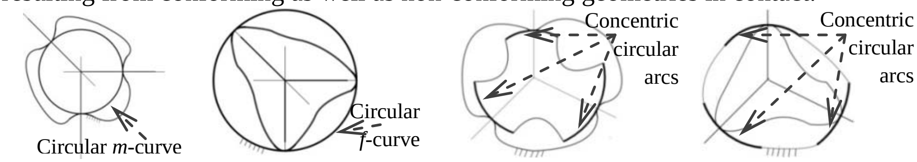

(a) Pure slipping full revolute pair. (b) Pure sliding full revolute pair. (c) Pure slipping partial revolute pair. (d) Pure sliding partial revolute pair.

Fig.12: Persistence of rotation center.

6 Conclusion

In this paper second-order mobility analysis of smooth planar contacting objects is studied using the geometries of contacting objects. It is shown that second order analysis results in partitioning of first order motion space along the contact normal line. A composition scheme using dual-number matrices is presented to handle multiple contacts mobility analysis. A novel contact vectors representation scheme helped determination of exact mobility regions through polygon intersection. It is established that non-trivial mobility region is a pair of open or a single closed convex polygon. The nature of the trivial mobility region is given by the intersection of contact vectors. The result led to systematic analysis of form closure and synthesis of revolute pairs which are impossible from first order analysis alone.

References

[1] F. Reuleaux, *The Kinematics of Machinery*. Macmillan, 1876, republished by Dover, NY (1963).

[2] M. T. Mason, *Mechanics of Robotic Manipulation*. MIT Press, Cambridge, MA (2001).

[3] E. Rimon and J. Burdick, "A Configuration space analysis of bodies in contact-II. 2nd order mobility," *J. Mech. Mach. Theory*, Vol.30, No.6, pp. 913-928, 1995.

[4] E. Rimon and J. Burdick, "Mobility of bodies in contact-Part I. A 2nd order mobility index for multiple-finger grasps," *IEEE Inter. Conf. on Robotics and Automation*, pp. 2329-2355, 1994.

[5] J. Takamatsu, H. Kimura and K. Ikeuchi, " Improved screw theory using second order terms," *Proc. of Inter. Conf. on Intelligent Robots and Systems*, pp. 1614-1618, 2002.